

EMULSION POLYMERIZATION TUBULAR REACTOR OF STYRENE WITH INTERNAL BAFFLES: VARIABLE REACTION TEMPERATURE

³Florentino L. Mendoza Marín and ²Liliane Maria Ferrareso Lona and ¹Rubens Maciel Filho
Faculty of Chemical Engineering, State University of Campinas (UNICAMP)

1. Laboratory of Optimization, Design and Advanced Process Control (LOPCA),
2. Laboratory of Analysis and Simulation of Chemical Process,
Department of Chemical Processes
- CP. 6066, CEP 13081-970, TL. +55 19 37883910, Campinas, SP, Brasil
3. E-mail: marin@lopca.feq.unicamp.br

Physicochemical, mathematical and computational sciences were used for the modeling and simulation of emulsion homopolymerization process of styrene with baffles into tubular reactor as static mixer. The objective is to model, to simulate and to analyze the emulsion polymerization reactor performance with internal-inclined angular baffles, and to compare with continuous tubular reactor in variable reaction temperature. Modeling and simulation were carried out steady state, considering cylindrical coordinate and one-dimensional model, fully developed laminar plug flow. The model was solved by finite volume method. Also it was considered the Smith-Ewart model to estimate the monomer conversion and Arrhenius chemical kinetics as laminar finite-rate model to compute chemical source. The experimental-inductive and mathematical-deductive methods were applied for obtaining mass balance results and properties characterization. The predictions were validated with experimental results for the isothermic and tubular reactor, with a good concordance. The results in no isothermal conditions with baffles were better than without baffles in relation to the desired properties.

Keywords: modeling, simulating, styrene, emulsion polymerization, tubular reactor, baffles.

1. Introduction

Plastics as synthetic polymers are mayor chemical industry goods used in the building, construction, packing, transportation, electronic, appliances, etc. Polymers are products of large importance in the current society with a market in significant expansion and the demands of products with required specifications by its applications. Polystyrene belongs to the group of standard thermoplastics, its annual consumption increase every year, it is one of the most important polymers, and its industrial production is carried out exclusively by a free radical mechanism. The fundamentals of emulsion polymerization are sufficiently well understood so that new products can be made, and old ones re-formulated. An example is the economically and technically importance to produce a submicron suspension of colloiddally stable polymer particles or latex with 40-50% by free radical mechanism of the total polymer. It is a heterogeneous reaction process in which unsaturated monomers or monomer solutions are dispersed in a continuous phase with the aid of an emulsifier system and polymerized with free-radical initiators (Paquet and Ray, 1994; Chern, 1995; Gilbert, 1995; Scholtens, 2002). Emulsion polymerization process is a complex heterogeneous process involving transport of monomer, free radicals and other species between aqueous and organic phases, compared to other heterogeneous polymerization (suspension or precipitation); it is likely the most complicated system. These entire factors make modeling of this system very difficult (Bockhorn, 1992; Gao and Penlidis, 2002).

The chemical processes in the chemical industry have growing operational difficulties caused by the diversification and specification of products and investigations for alternative reactors projects, analysis of their behavior under static and dynamic conditions are wellcome. In conventional tubular reactor (TR), the most reaction happens towards the reactor entrance, and the variable reaction for exothermic reactions as well as the limitations to heat transfer near the wall makes the behavior to be very complex (Maciel Filho e Domingues, 1992; Siirola, 1996; Kiparissides, 1996, Toledo, 1999).

The emulsion homopolymerization of styrene was considered and a steady-state one-dimensional model was developed to simulate the system. The model is written in cylindrical coordinate with the hypothesis of fully developed laminar plug flow and solved with finite volume method (FVM). In fact conventional TR may have serious limitations to heat transfer leading to the obtation of product with undesired conditions. Bearing this in mind in this work it is proposed an alternative TR based on the placement of the baffles inside the reactor for emulsion polymerization of styrene (EPS). The objective is to model, simulate and analyze the emulsion polymerization reactor performance with internal inclined angular baffles on variable reaction temperature effect. Attention is give for conversion, number of particles, molecular weight distribution and particle size. The products were characterized with particles number (homogeneous and heterogeneous nucleation), molecular weight distribution, polymer particles size and polymer viscosity distribution. These results were validated with literature results under same or approximate condition. The results in no isothermal conditions with baffles were better than without baffles in relation to the desired properties. The methodology will be treated like reactional system, mathematical modeling and numerical method.

2. Reactional System

2.1 Conditions of test

In order to evaluate the performance of the proposed design the EPS is considered, comparison with conventional TR is carried out. Figure 1 shows the alternative proposed reactor. To represent the system a simplified one dimensional deterministic model is developed with the following assumptions: flow along the axial direction (negligible diffusion), fully developed axial velocity of fluid flow, polymer particle phase is the main locus of polymerization, particle size is monodisperse, the monomer conversion is estimated by Smith-Ewart model, and Arrhenius chemical kinetics as laminar finite-rate model to compute chemical source.

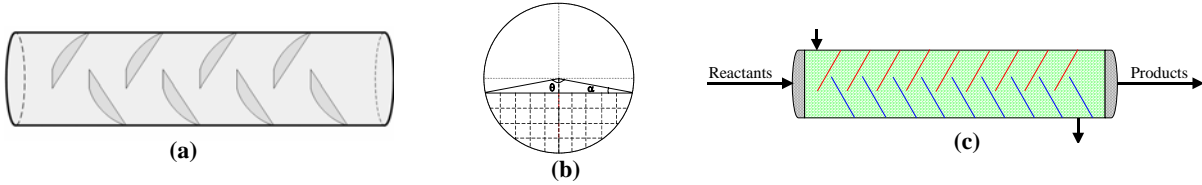


Figure 1 (a) Schematic representation of polymerization TR with baffles, (b) Variation of transversal area of fluid flow of EPS and (c) Profile of polymerization TR with internal-inclined angular baffles.

2.2 Properties

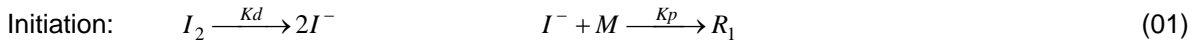
In order to evaluate the performance of the proposed alternative reactor design the EPS was considered specifically the work of BATAILLE *et al.* (1982) that conducted emulsion homopolymerization of styrene at 60°C with the potassium persulfate, 0.026 (mol/L), Sodium dodecyl sulfate, 0.070 (mol/L), styrene, 8.39 (mol/L) and water, 161.52 (mol/L), it was taken as case study. The bibliographical references of the properties and parameters of the Table 1 can be found in Mendoza Marín (2004).

3. Mathematical Modeling

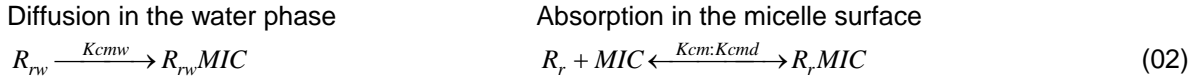
In order to represent the proposed reactor shown in Figure 1, with the case study of emulsion homopolymerization of styrene the following model equation may be written.

3.1 Chemical Reaction

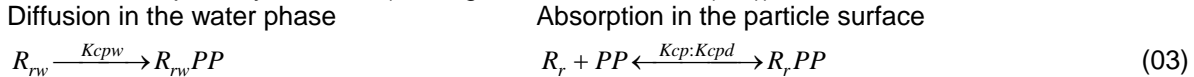
The mechanism of EPS may schematic and brief shown as:



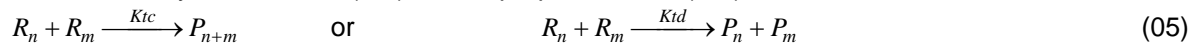
Radical Absorption by Micelles (Micellar Nucleation (MN))



Radical Absorption by Particles (Homogeneous Nucleation (HN))



Termination: by combination (Ktc) and disproportionation (Ktd)



3.2 Conservative Models

Principle of Mass Conservation in general form for a chemical species j reacting in a flowing fluid with varying density, temperature, and composition is

$$\frac{\partial C_j}{\partial t} + \nabla \cdot (C_j \bar{u}) + \nabla \cdot J_j = R_j \quad (06)$$

where C_j is the molar concentration of species j ; $\partial C_j / \partial t$ is the nonsteady-state term expressing accumulation or depletion; ∇ is the gradient operator; $\nabla \cdot \bar{u}$ is the divergence of a vector function \bar{u} ; \bar{u} is the three-dimensional mass-average velocity vector; $\nabla \cdot (C_j \bar{u})$ is the transport of mass by convective flow; J_j is the molar flux vector for species j with respect to the mass-average velocity; $\nabla \cdot J_j$ is molecular diffusion only; R_j is the total rate of change of the amount of j because of reaction. Species j occurs in liquid phase. This equation can take in single-phase or "homogeneous" or "pseudohomogeneous" reactors (Bird, 1960; Froment, 1990).

The generalized *Laminar Finite-rate Model* was applied to compute the chemical source terms (R_j). The model is exact for laminar flames, but is generally inaccurate for turbulent flames due to highly non-linear

Table 1: Physics, chemicals, mechanics, transport, rheologys, thermodynamics, geometrical properties (grid, particles, reactor, baffles) properties of Styrene as database for simulation of EPS.

Symbol	Value, Unit and Description
Na	6.02x10 ²³ (molecule/mol); Abogadro's number; $\pi = 3.14159$
Rg	1.987 (cal/mol K); gas constant
ρ_p, ρ_m	1.25-0.0004202T (Kg/L), polymer and 0.949-0.00128(T-273.15); (Kg/L), monomer density
anrp	0.5; average number of radicals per particle
CMC	0.008 (mol/L); critical micelle concentration
CMw	0.005 (mol/L); monomer concentration in water phase (=Mw)
fi	0.5; initiator efficiency
Kcm	4 π Dwr _{mic} N _A (1/min); rate const of aqueous phase radical capture by micelles
Kcp	4 π Dpr _p N _A (1/min); rate const of radicals capture by polymer particles
Kd	1.524x10 ¹⁸ exp(-33320/RgT) (1/min); rate constant of initiator decomposition
Kp	4.703x10 ¹¹ exp(-9805/RgT) (L/mol min); rate const. of propag. of poly. partis
Kt	1.04619x10 ¹⁰ exp(-2950,45/RgT) (L/mol min); global rate const for termination
[M] _p	(1- ϕ_p) ρ_m /MWs (mol/L); monomer concentration in polymer particle
MWe	288.38 (g/mol); molecular weight of surfactant
MWi	271.3 (g/mol); molecular weight of initiator
MWs	104 (g/mol); molecular weight of styrene
ncr	5; critical chain length at which water phase radical can be absorbed
nem	60 (No.Emul/mic); number of emulsifier molecules in a micelle
Sa	3x10 ⁻¹⁷ (dm ²); area covered by one molecule of emulsifier
ϕ_p, ϕ_m	0.4, volume fraction of polymer; 0.6, volume fraction of monomer
Re	5000 (laminar) and 13600 (turbulent) Reynolds number
Vin	0.27027 (laminar) and 0.7351 (turbulent) (m/min) inlet velocity in TR
Dp	1.76x10 ⁻¹² (dm ² /min); (diffusivity of monomer radicals in polymer phase
Dw	1.76x10 ⁻⁹ (dm ² /min); (diffusivity of monomer radicals in water phase
μ	0.001 (Kg/m s); viscosity of polymer
Tin	333.15 and 363.15 (K); inlet temperatures to the reactor
ΔH	-16682.2 (cal/mol); polymerization reaction heat of styrene
N	51; number of nodal points
r _{mic} , r _p	27.5 (Å); radius of micelle and 275 (Å); radius of polymer
Dr, Lr	1 (m) diameter and 20 (m) length of TR
Lbr	1 (m) length of baffle separation and Nb = 6, 18 number of baffles

Arrhenius chemical kinetics. The net source of chemical species j due to reaction R_j is computed as the sum of the Arrhenius reaction sources over the N_i reactions that the species participate in:

$$R_j = \sum_{i=1}^{N_i} R_{j,i} = \sum_{i=1}^{N_i} \left(K_{f,i} \prod_{j=1}^{N_i} [C_{j,i}]^{n_{fj,i}} - K_{b,i} \prod_{j=1}^{N_i} [C_{j,i}]^{n_{bj,i}} \right) \quad (07)$$

where $R_{j,i}$ is the Arrhenius molar rate of creation/destruction of species j in reaction i ; $K_{f,i}$ is the forward rate constant for reaction i , $K_{b,i}$ is the backward rate constant for reaction i , N_i is the number of chemical species in reaction i , $C_{j,i}$ is the molar concentration of each reactant and product species j in reaction i , $n_{fj,i}$ is the forward rate exponent for each reactant and product species j in reaction i , $n_{bj,i}$ is the backward rate exponent for each reactant and product species j in reaction i . Only non-reversible reactions was considered and the mass balance of equations gives the different chemical source term as free radical (R_{Rw}), initiator (R_I), monomer (R_M), surfactant ($R_E=0$, by to be inert), and polymer (R_P):

$$R_{Rw} = R_I - R_I \left[\frac{K_p M_w}{K_p M_w + K_{cp} [N_p] + K_{tw} [R]_w} \right]^{ncr-1} - K_{cp} [N_p] [R]_w - K_{cm} [MIC] [R]_w - K_{tw} [R]_w^2 \quad (08)$$

$$R_I = -fiKd[I]_w; R_M = -\frac{K_p [M]_p N_p \bar{n}}{N_A V_p} - K_{pw} [M]_w [R]_w; R_P = \frac{K_p [M]_p N_p \bar{n}}{N_A V_p} + K_{pw} [M]_w [R]_w \quad (09)$$

Newton's Second Law of Momentum was applied to a small volume element moving with the fluid that is accelerated because the forces acting over it. The motion equation in terms of τ is

$$\rho \frac{D\vec{u}}{Dt} = -\nabla P + (\nabla \cdot \vec{\tau}) + \rho \cdot \vec{g} \quad (10)$$

here \vec{g} represent the body force per unit area; ρ is the density; P is the pressure; $\vec{\tau}$ is the extra stress tensor, and D/Dt is the material or substantial derivative (Bird, 1960; Tucker, 1989; Versteeg, 1998).

Principle of Energy Conservation in the following form shows the phenomenon that are of importance in reactors is

$$\sum_j \bar{M}_j C_j c_{pj} \left(\frac{\partial T}{\partial t} + \vec{u} \cdot \nabla T \right) = \sum_i (-\Delta H_i) r_i + \nabla \cdot (\lambda \nabla T) - \sum_j J_j \nabla H_j + Q_{rad} \quad (11)$$

where c_{pj} is the specific heat of species j ; λ is the thermal conductivity of the mixture; H_j are partial molar enthalpies; T is the temperature; \bar{M}_j is molecular mass of species j ; Q_{rad} is heat of radiation (Froment, 1990).

In the *Micellar Nucleation* (MN) is accepted that particles are generated by micelle absorbing radicals from the water phase where R_{MN} is the rate of particle formation by MN (see mechanism).

$$R_{MN} = \frac{d[Np]_m}{dt} = K_{cm}[MIC][R]_w \quad (12)$$

Formation rate for the 1st oligomeric radicals in the aqueous phase (see Mechanism) is

$$\frac{d[R_1]_w}{dt} = R_I - K_p M_w [R_1]_w - K_{cm}[MIC][R_1]_w - K_{tw}[R]_w [R_1]_w \quad (13)$$

Formation rate for the i th oligomeric radicals in the aqueous phase (see Mechanism) is

$$\frac{d[R_i]_w}{dt} = K_p M_w [R_{i-1}]_w - K_p M_w [R_i]_w - K_{cm}[MIC][R_i]_w - \sum_{j=1}^{\infty} K_{cp_j} [Np_j] [R_i]_w - K_{tw} \sum_{j=1}^{ncr-1} [R_i]_w [R_j]_w \quad (14)$$

$$\text{Definition: } \sum_{j=1}^{\infty} K_{cp_j} [Np_j] = K_{cp} [Np] \quad (15)$$

Formation rate of total oligomeric radicals in the aqueous phase ($[R]_w$)

$$\sum_{j=1}^{ncr-1} [R_j]_w = [R]_w \quad (16)$$

If the steady state hypothesis is applied to all radicals in the water phase, i.e., setting left-hand side of Eq.(13) and Eq.(14) to zero, one obtain the following equations:

$$[R_1]_w = \frac{R_I}{K_p M_w + K_{cm}[MIC] + K_{tw}[R]_w} \quad (17)$$

$$[R_i]_w = \frac{K_p M_w [R_{i-1}]_w}{K_p M_w + K_{cm}[MIC] + K_{tw}[R]_w + K_{cp} [Np]} \quad (18)$$

The probability for oligomeric radical for micelle propagation (α_m)

$$\alpha_m = \frac{K_p M_w}{K_p M_w + K_{cm}[MIC] + K_{tw}[R]_w + K_{cp} [Np]} \quad (19)$$

Equation (18) can then be rewritten and solve for all oligomer

$$[R_i]_w = \alpha_m [R_{i-1}]_w = \alpha_m \alpha_m [R_{i-2}]_w = \alpha_m \alpha_m \alpha_m [R_{i-3}]_w = \dots = \prod_{i=1}^{ncr-1} \alpha_m^i [R_1]_w \quad (20)$$

$$[R_i]_w = \alpha_m^{ncr-1} [R_1]_w \quad (21)$$

Substituting Eq.(17) into Eq.(21) gives

$$[R_i]_w = \frac{R_I}{K_p M_w + K_{cm}[MIC] + K_{tw}[R]_w} \alpha_m^{ncr-1} \quad (22)$$

The following definitions are used to simplify symbols. Total radical concentration in the aqueous phase

$$[R]_w = \sum_{i=1}^{ncr-1} [R_i]_w \quad (23)$$

Substituting Eq.(22) into Eq.(23) gives

$$[R]_w = \frac{R_I}{K_p M_w + K_{cm}[MIC] + K_{tw}[R]_w} \sum_{i=1}^{ncr-1} \alpha_m^{ncr-1} \quad (24)$$

The Geometric Progression is applied to the end term of Eq.(24)

$$\sum_{i=1}^{n-1} x^{i-1} = \frac{1 - x^{n-1}}{1 - x} \quad (25)$$

Equation (24) can be then rewritten an gives the total radical concentration in the aqueous phase.

$$[R]_w = \frac{R_I}{K_p M_w + K_{cm}[MIC] + K_{tw}[R]_w} \left(\frac{1 - \alpha_m^{ncr-1}}{1 - \alpha_m} \right) \quad (26)$$

The final equation of the rate of particle formation for MN is then

$$R_{MN} = \frac{d[Np]_m}{dt} = \frac{K_{cm}[MIC]R_I}{K_pM_w + K_{cm}[MIC] + K_{tw}[R]_w} \left(\frac{1 - \alpha_m^{ncr-1}}{1 - \alpha_m} \right) \quad (27)$$

In the *Homogeneous Nucleation* (HN) is accepted that the particles could be generated by precipitated water phase oligomer radicals where R_{HN} is the rate of particle formation by HN (see mechanism).

$$R_{HN} = \frac{d[Np]_h}{dt} = K_pM_w [R_{ncr-1}]_w \quad (28)$$

Formation rate for 1st oligomeric radicals in the aqueous phase (see Mechanism)

$$\frac{d[R_1]_w}{dt} = R_I - K_pM_w [R_1]_w - \sum_{j=1}^{\infty} K_{cpj} [Np_j] [R_1]_w - K_{tw} \sum_{j=1}^{ncr-1} [R_j]_w [R_1]_w \quad (29)$$

Formation rate for *i*th oligomeric radicals in the aqueous phase (see Mechanism)

$$\frac{d[R_i]_w}{dt} = K_pM_w [R_{i-1}]_w - K_pM_w [R_i]_w - K_{cp} [Np] [R_i]_w - K_{tw} [R]_w [R_i]_w \quad (30)$$

If the steady state is applied to all radical in the water phase, the following equation was obtained:

$$[R_1]_w = \frac{R_I}{K_pM_w + K_{cp}[Np] + K_{tw}[R]_w} \quad (31)$$

$$[R_i]_w = \frac{K_pM_w [R_{i-1}]_w}{K_pM_w + K_{tw}[R]_w + K_{cp}[Np]} \quad (32)$$

The probability for an oligomeric radicals for homogeneous propagation (α_h)

$$\alpha_h = \frac{K_pM_w}{K_pM_w + K_{tw}[R]_w + K_{cp}[Np]} \quad (33)$$

Equation (31) and Eq.(32) can then be rewritten and solve for all radical oligomer

$$[R_1]_w = \frac{R_I}{K_pM_w} \alpha_h \quad (34)$$

$$[R_i]_w = \alpha_h [R_{i-1}]_w = \alpha_h \alpha_h [R_{i-2}]_w = \alpha_h \alpha_h \alpha_h [R_{i-3}]_w = \dots = \prod_{i=1}^{ncr-1} \alpha_h^i [R_1]_w \quad (35)$$

Substituting Eq.(34) into Eq.(35) gives

$$[R_i]_w = \alpha_h^{ncr-1} [R_1]_w = \frac{R_I}{K_pM_w} \alpha_h^{ncr} \quad (36)$$

Definition of radicals where chain length at the *critical chain length* (*ncr*). The last propagation step involving a radical of chain length *ncr-1* and a monomer can actually be considered as the particle formation step (Gilbert, 1995; Gao and Penlidis, 2002). Applying this definition to Eq. (36) gives

$$[R_{ncr-1}]_w = \frac{R_I}{K_pM_w} \alpha_h^{ncr-1} \quad (37)$$

Substituting Eq.(37) into Eq.(28) gives the final equation of the rate of particle formation by HN:

$$R_{HN} = \frac{d[Np]_h}{dt} = R_I \alpha_h^{ncr-1} \quad (38)$$

3.3 Characterization of Polymer Particle

The polymer particle (by MN and HN) is determined with Eq. (06) written like Eq. (39) and source term as Eq. (40):

$$\frac{\partial C_{N_p}}{\partial t} + \left(v_r \frac{\partial C_{N_p}}{\partial r} + v_\theta \frac{1}{r} \frac{\partial C_{N_p}}{\partial \theta} + v_z \frac{\partial C_{N_p}}{\partial z} \right) = D_{NB} \left(\frac{1}{r} \frac{\partial}{\partial r} \left(r \frac{\partial C_{N_p}}{\partial r} \right) + \frac{1}{r^2} \frac{\partial^2 C_{N_p}}{\partial \theta^2} + \frac{\partial^2 C_{N_p}}{\partial z^2} \right) + R_{N_p} \quad (39)$$

$$R_{N_p} = R_{MN} + R_{HN} = \frac{K_{cm}[MIC]R_I}{K_pM_w + K_{cm}[MIC] + K_{tw}[R]_w} \left(\frac{1 - \alpha_m^{ncr-1}}{1 - \alpha_m} \right) + R_I \alpha_h^{ncr-1} \quad (40)$$

The *Molecular Weight Distribution* is determined with mechanism of EPS, discrete transformation method, this method include the steps of chemical reaction, kinetic equation, integrating, expand in power series, drop operator, and moments. Generating function solved the kinetic equations. The *Cumulative Dead Polymer* were number-average molecular weight (M_n^c) and weight-average molecular weight (M_w^c):

$$M_n^c = \frac{2aMW_s}{a-b} \frac{X_j}{\ln\left(\frac{b-aX_j}{b}\right)} \quad M_w^c = MW_s \left(\frac{a+2b}{b-a} - \frac{3a}{2(b-a)} X_j \right) \quad (41)$$

$$\text{where} \quad a = Kp[M] \quad b = a + Ktc[R]_w \quad (42)$$

The average swollen (R_s) and unswollen (R) *particle polymer size radius* (Paquet and Ray, 1994) are

$$R_s = \left(\frac{3}{4\pi\rho_p\phi_p} \frac{MW_p C_{Ps}}{N_A C_{Np}} \right)^{1/3} \quad R = R_s \left(\frac{\rho_m}{\rho_m + [M]_p MW_m} \right)^{-1/3} \quad (43)$$

The viscosity of polymer (μ) was estimated (Harkness, 1982) as:

$$\ln(\mu) = -13,04 + \frac{2013}{T} + MW_p^{0,18} \left[3,915X_j - 5,437X_j^2 + \left(0,623 + \frac{1387}{T} \right) X_j^3 \right] \quad (44)$$

3.4 Reactor and Baffle: geometry effect

The *internal transversal areas over or beneath baffles* were calculated where α is the increment angle from the TR center point until total diameter, θ is the increment angle to calculate the fluid flow area of EPS beneath or over the baffles, Avb is fluid flow variable area inside TR beneath or over baffles, Ar is the area of TR without baffles and Afb is the fixed area inside TR over or beneath baffles (Figure. 1 (b)).

$$\alpha r(1) = \text{arcSen} \left(2 \frac{ID(1)}{Dr} \right) \quad [\text{rad}] \quad (45)$$

$$\theta r(1) = \frac{\pi}{180} \theta g(1) = \pi \left(1 - 2 \frac{\alpha r(1)}{\pi} \right) \quad [\text{rad}] \quad (46)$$

$$Avb(1) = \frac{Dr^2}{8} (\theta r(1) - \text{Sen} \theta r(1)) \quad (47)$$

$$Afb(1) = Ar - Avb(1) = \frac{\pi}{4} Dr^2 - Avb(1) \quad (48)$$

Calculus of Avb from $l=2$ to Number of areas beneath or over baffles (Nab)

$$Dvb(I) = Dvb(I-1) + \Delta Dvb \quad (49)$$

$$\alpha r(I) = \text{arcSen} \left(2 \frac{ID(I)}{Dr} \right) = \text{arcSen} \left(\frac{2}{Dr} (Dvb(I) - 0.5 * Cr) \right) \quad (50)$$

$$\theta r(I) = \frac{\pi}{180} \theta g(I) = \pi \left(1 - \frac{2}{\pi} \alpha r(I) \right) \quad (51)$$

$$Afb(I) = \frac{Dr^2}{8} (\theta r(I) - \text{Sen} \theta r(I)) \quad (52)$$

$$Avb(I) = Ar - Afb(I) \quad (53)$$

The *axial velocity* like at TR inlet over or beneath baffles and temperature effects were estimated from Newton's Second Law of Momentum and continuity equation where v_{in} is the axial velocity at TR inlet in isothermal condition, v_b is the axial velocity over or beneath baffles in isothermal condition and v_z is the axial velocity in no isothermal condition.

$$v_{in} = \frac{\mu R_e}{\rho D_r} \quad v_b = \frac{\mu A_r R_e}{\rho A_{vb} D_r} \quad v_z = \frac{v_{zo} \rho_o}{\rho} \quad (54)$$

4. Numerical Method

Finite Volume Method was used as numerical method according with Patankar (1980), Maliska (1995), and Versteeg (1998). The *Discrete approximation* was applied to conservative balance of convection and source only, e.g. the equation of particle number, Eq. (39) and source term or the overall rate of formation of particles by MN and HN, Eq. (40). The *Linear approximation* was applied to source term of Eq. (39). The Taylor's Series method of linearization was used for to linearize S_ϕ . The overall equation of source-term linearization, ($S_\phi = S_{Np}$) in Eq. (40) leads to

$$S_{Np} = R_{Np} = S_{Npm} + S_{Nph} = SUT - SPT[Np]_p \quad (55)$$

Source-term linearization for *Micellar Nucleation* (S_{Npm}) in Eq. (27) allows to write:

$$S_{Npm} = SUM - SPM[Np]_p \quad (56)$$

Taylor's Series for one variable was applied to linearizar the source-term, Eq.(27)

$$S_{Npm}([Np]) = S_{Npm}([Npa]) + S'_{Npm}([Npa])([Np] - [Npa]) \quad (57)$$

$$SUM = SUM1 + SUM2 - SUM3 \quad (58)$$

$$SUM1 = m4 \left(\frac{m3 + Kcp[Npa]}{m2 + Kcp[Npa]} \right) \left(1 - \left(\frac{m1}{m3 + Kcp[Npa]} \right)^{ncr-1} \right) \quad (59)$$

$$SUM2 = \left(\frac{m1m4Kcp[Npa]}{(m2 + Kcp[Npa])^2} \right) \left(1 - \left(\frac{m1}{m3 + Kcp[Npa]} \right)^{ncr-1} \right) \quad (60)$$

$$SUM3 = \left(\frac{(ncr-1)m4Kcp[Npa]}{m2 + Kcp[Npa]} \right) \left(\frac{m1}{m3 + Kcp[Npa]} \right)^{ncr-1} \quad (61)$$

$$\text{where: } m1 = KpMw, \quad m2 = Kcm[MIC] + Ktw[R]_w, \quad m3 = m1 + m2, \quad m4 = \frac{Kcm[MIC]R_I}{m3} \quad (62)$$

The following definitions are used to simplify the coefficient SPM of Eq.(57)

$$SPM = SPM1 - SPM2 \quad (63)$$

$$SPM1 = \left(\frac{m1m4Kcp}{(m2 + Kcp[Npa])^2} \right) \left(1 - \left(\frac{m1}{m3 + Kcp[Npa]} \right)^{ncr-1} \right) \quad (64)$$

$$SPM2 = \left(\frac{(ncr-1)m4Kcp}{m2 + Kcp[Npa]} \right) \left(\frac{m1}{m3 + Kcp[Npa]} \right)^{ncr-1} \quad (65)$$

Source-term linearization for *Homogeneous Nucleation* (S_{Nph}) in Eq. (38) is

$$S_{Nph} = SUH - SPH[Np]_p \quad (66)$$

Taylor's Series for one variable was applied to linearize the source-term, Eq.(38)

$$S_{Nph}([Np]) = S_{Nph}([Npa]) + S'_{Nph}([Npa])([Np] - [Npa]) \quad (67)$$

$$SUH = SUH1 + SUH2 \quad (68)$$

$$SUH1 = R_I \left(\frac{h1}{h2 + Kcp[Npa]} \right)^{ncr-1} \quad (69)$$

$$SUH2 = \frac{(ncr-1)KcpR_I[Npa]}{h1} \left(\frac{h1}{h2 + Kcp[Npa]} \right)^{ncr} \quad (70)$$

$$\text{where: } h1 = KpMw, \quad h2 = h1 + Ktw[R]_w \quad (71)$$

The following definition is used to simplify the coefficient SPH of the Eq.(67)

$$SPH = \frac{(ncr-1)KcpR_I}{h1} \left(\frac{h1}{h2 + Kcp[Npa]} \right)^{ncr} \quad (72)$$

Now we sum the Eq.(39) and Eq.(69) to obtain the coefficient SUT of the Eq.(56)

$$SUT = SUM + SUH \quad (73)$$

Now we sum the Eq.(64) and Eq.(73) to obtain the coefficient SPT of the Eq.(56)

$$SPT = SPM + SPH \quad (74)$$

Now the *integral form* of general transport equations in one-dimensional control volume is given by:

$$\int_{cv} \frac{\partial(v_z Np)}{\partial z} Adz = \int_{cv} S_{Np} Adz = \int_{cv} (SUT - SPT.Np_p) Adz \quad (75)$$

$$(AvNp)_e - (AvNp)_w = (S_{Np}Az)_e - (S_{Np}Az)_w = (SUT - SPT.Np_p)A_p \Delta z \quad (76)$$

The continuity Equation is:

$$(Av\rho)_e = (Av\rho)_w \quad (77)$$

In the *interpolation* was applied the upwind difference scheme to calculate the particle number as:

$$F_w \phi_w = \phi_w \|F_w, 0\| - \phi_P \|F_w, 0\| \quad F_e \phi_e = \phi_P \|F_e, 0\| - \phi_E \|F_e, 0\| \quad (78)$$

$$\text{where: } F = \rho v \quad (79)$$

Mass Balance or continuity equation

$$A_w \|F_w, 0\| = A_w \|F_w, 0\| - A_w F_w \quad A_e \|F_e, 0\| = A_e \|F_e, 0\| + A_e F_e \quad (80)$$

After integration and interpolation were obtained the *linear algebraic equations*. In the minimum control volume the discretised equation for minimum control volume is

$$a_p Np_p = a_E Np_E + S_U \quad (81)$$

$$\text{where: } a_W = 0, a_{in} = A_w \|F_w, 0\|, a_E = A_e \| -F_e, 0\|, a_P = a_E + S_P \quad (82)$$

$$S_P = SPT.A_P \Delta z + a_{in} + (A_e F_e - A_w F_w), S_U = SUT.A_P \Delta z + a_{in} N_{pin} \quad (83)$$

In the internal control volume from $l=3$ to $l=N-2$, the discretised equation for internal control volume is

$$a_P N_{p_P} = a_W N_{p_W} + a_E N_{p_E} + S_U \quad (84)$$

$$\text{where: } a_W = A_w \|F_w, 0\|, a_E = A_e \| -F_e, 0\|, a_P = a_W + a_E + S_P \quad (85)$$

$$S_P = SPT.A_P \Delta z + (A_e F_e - A_w F_w), S_U = SUT.A_P \Delta z \quad (86)$$

In the maximum control volume $l=N-1$, the discretised equation for maximum control volume

$$a_P N_{p_P} = a_E N_{p_E} + S_U \quad (87)$$

$$\text{where: } a_W = A_w \|F_w, 0\|, a_E = 0, a_P = a_W + S_P \quad (88)$$

$$S_P = SPT.A_P \Delta z + (A_e F_e - A_w F_w), S_U = SUT.A_P \Delta z \quad (89)$$

The *solution of discretized algebraic equations* were obtained by Thomas Algorithm or the Tri-diagonal Matrix Algorithm (TDMA) as direct method for one-dimensional situation problems; they were the initiator, radicals, number of particle, monomer, polymer and temperature. The iterative procedures were used in digital computers for solving systems of discretized linear algebraic equations like Eq.(82), Eq.(85) and Eq.(88), and we shall solve the set of such equations by the method for linear algebraic equations. The convergence problem is to find number of particle and temperature. We shall handle such situations by iteration. This process involves the following steps with or without baffles: 1) Start with a guess or estimate value of aN_p and aT for all grid points; 2) From these guessed aN_p 's and aT 's, calculate the coefficients of the discretized equations of initiator, radicals, number of particle and temperature; 3) Solve the nominally linear set of algebraic equations to get new values of N_p ; 4) With these N_p 's as better guesses, return to step 2 and repeat the process until absolute value of $|N_p - aN_p|$ is lower than a factor of convergence; 5) Calculate the temperature T with number of particle N_p of step 4; 6) With these T 's as better guesses, return to step 2 and repeat the process until absolute value of $|T - aT|$ is lower than a factor of convergence.

5. Results and Discussion

The simulation results of **conversion** (X_j) versus length of the reactor (Z) for styrene without baffle (V0) and with baffles (V6) in no isothermal condition (V) are displayed in Figure 2 (a). The conversion with $N_b=6$ baffles show better results that the conversion without baffles. When the baffle numbers is increased, the conversion increase. The comparative results in isothermal condition at 60°C of computational conversion (X_{cC}), experimental conversion (X_e), and simulation conversion (literature results) (X_s) versus residence time (t) inside TR are shown in Figure 2 (b). The experimental conversion has equal isothermal temperature and properties as computational conversion but the simulation conversion has different mathematical model. The experimental and simulation conversion was used of Bataile et al. (1982). It can be observed that the three curves have same behavior. These comparisons prove the validation of FVM through the comparative of experimental and simulation results.

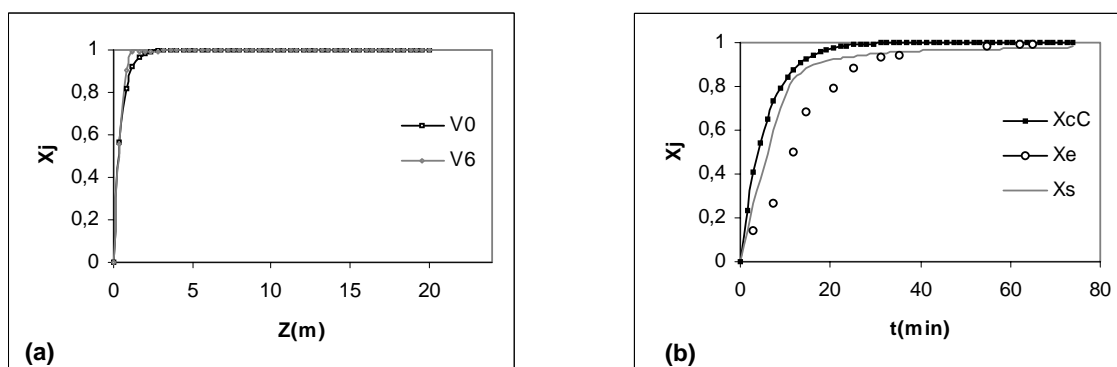


Figure 2 (a) Conversion of monomer without ($N_b=0$) and with ($N_b=6$) baffles in no isothermal ($V_{N_b=T}$) and (b) experimental validation in isothermal conditions (60°C).

The simulation results of the **polystyrene particles number** (N_p) by MN and HN mechanism versus length of the reactor (Z) without (V0) and with ($N_b=6$) baffles in no isothermal condition (V) were shown in Figure 3 (a). The two curves show augment when temperature varies in axial TR. The experimental (N_{pe}) and simulation (N_{ps}) of the particle numbers without baffles inside batch reactor versus time (t) is

expounded in Figure 3 (b). Its experimental and simulation conditions are feed temperature of 50°C, potassium persulfate (KPS) 0,011 mol/l, sodium dodecyl sulfate (SDS) 0,05 mol/l, and no adiabatic process. De la Rosa et al. (1996) indicated in relation to the Figure 3 (b) that the experiment results is in a close range within experimental measurement error, considering the difficulty associated with particle number measurement determination, the model prediction should be considered satisfactory. The particle number of the model prediction is approximately at $1,28 \times 10^{18}$ 1/L as shown in Figure 3 (b). The comparison of the two figures prove principally validation of the mathematical model and numerical method of FVM, nevertheless the difference in both figures would be by use of different simulation conditions. This comparison is better without baffles as shown in curve V0 of the Figure 3 (b).

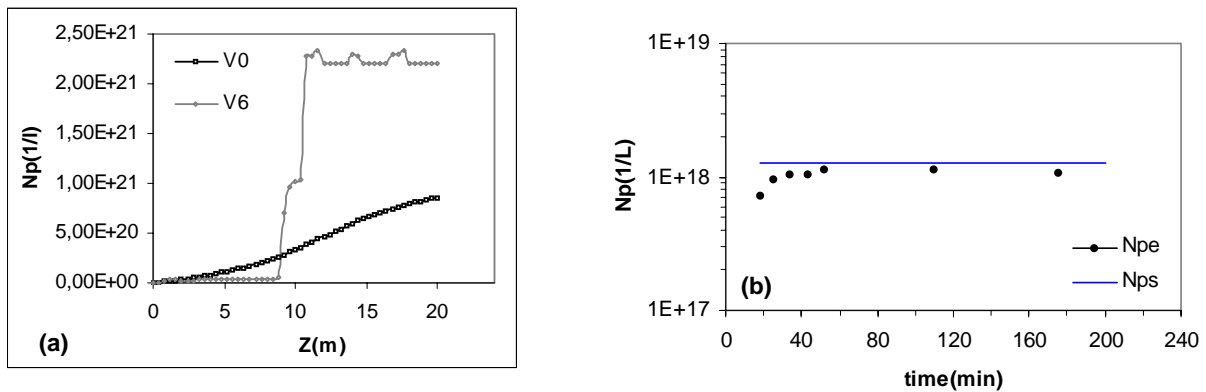


Figure 3 (a) Number of particles without ($Nb=0$) and with ($Nb=6$) baffles in no isothermal ($VNb=T$) conditions and (b) Number of particle validation at isothermic condition.

The results of simulation of the cumulative average **molecular weight distribution** versus conversion of monomer (X_j), without baffle ($MnV0$, $MwV0$) and with baffles ($MnV6$, $MwV6$) in variable reaction temperature through of TR are shown in Figure 4. The average molecular weights as shown in Figures 4 (a) and (b) have different performance by reaction temperature effect. The number (Mn) and weight (Mw) molecular improve its distribution when the baffles number increase inside TR. The results of molecular weigh distribution were obtained with the results of initiator, radicals, conversion, particle numbers, etc., e.g. the conversion that was validated with experimental results as shown in Figure 2(b).

The comparative results of simulation of the **polystyrene particles size** of unswollen particle radius (R) versus length of the reactor (Z) without ($V0$) and with ($V6$) baffles in no isothermal condition (V) are presented in Figure 5 (a). The particle size without baffles shows the highest size than with $Nb=6$ baffles. Both curve $V0$ and $V6$ have similar behavior according the temperature increment. When the baffle numbers increase in reactor, the particle size diminishes its size.

The simulation results of **polymer viscosity distribution** ($\ln(\mu)$) inside TR versus conversion of monomer (X_j) without baffle ($V0$) and with baffles ($V6$) in no isothermal condition is shown in Figure 5 (b). The two curves have some similar behavior when increase the baffles number, but the viscosity with $Nb=6$ baffles is lower than the viscosity without baffles. The mathematical model of the Eq.(44) was used for estimate the viscosity of the two curves (Harkness, 1996).

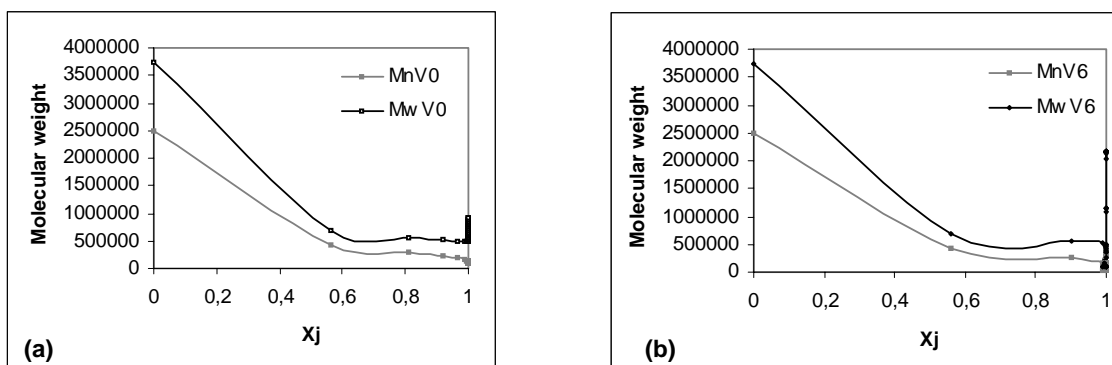


Figure 4 Molecular weight distribution (a) without ($Nb=0$) and (b) with ($Nb=6$) baffles in no isothermal conditions ($VNb=T$).

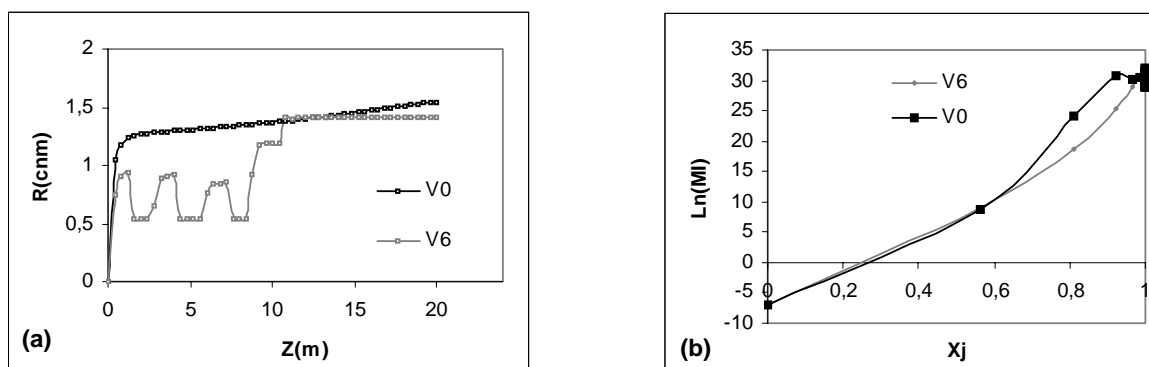


Figure 5 (a) Average particle size distribution and (b) viscosity distribution, both without ($Nb=0$) and with ($Nb=6$) baffles in no isothermal conditions ($VN_b=T$).

6. Conclusions

The performances of emulsion polymerization reactor in no isothermal condition shown better results when the baffles number were increased inside tubular reactor. In particular the conversion and particle number increase when the baffles numbers were increased inside tubular reactor and it were compared to the conventional tubular reactor. On the other hand the particle size and viscosity decrease when they increase the baffle number. A better molecular weight distribution is obtained for new proposed reactor. In general the results for the no isothermal condition with baffles are better than the reactor without baffles in relation to desired properties.

7. Acknowledges

The author is grateful to the PEC-PG/CAPES and LOPCA-DPQ/FEQ UNICAMP for their financial support.

8. Bibliography

- BOCKHORN, H., *Mathematical Modeling*, ULLMANN'S Encyclopedia of Industrial Chemistry, Vol.B1, 2, 1992.
- CHERN, C.S., *Diffusion-Controlled semibatch Emulsion Polymerization of Styrene*; *Journal of Applied Polymer science*, Vol.56, 221-230, 1995.
- FARINAS, M.I., GARON, A. e LOUIS, K.S., *Study of heat transfer in a horizontal cylinder with fins*, *Ver. Gen. Therm*, 36, 398-410, 1997.
- FROMENT, G.F. AND BISCHOFF, K.B.; *Chemical Reactor Analysis and Design*; Second Edition; John Willey-Sons; 1990.
- GAO, J. AND PENLIDIS, A.; *Mathematical Modeling and Computer Simulator/database for Emulsion Polymerizations*; *Prog. Polym. Sci.* ;27, 403-535, 2002.
- GILBERT, R.G.; *Emulsion Polymerization, A Mechanistic Approach*; Academic Press; London; 1995.
- HARKNESS, M.R. *A computer simulation of the bulk polymerization of polystyrene in a tubular reactor*. M.S. Thesis, Rensselaer Polytechnic Institute, Troy, New York, 1982.
- KIPARISSIDES, C. *Polymerization Reactor Modeling: A Review of Recent Developments and Future Directions*. *Chemical Eng. Science*, Vol.51, No.10, 1996.
- MACIEL FILHO, R., and DOMINGUES, A., *Multitubular Reactor for Obtención of Acetaldehyde by Oxidation of Ethyl Alcohol*, ISCRE 12 (Twelfth International Symposium on Chemical Reaction Engineering), Turin, Itália, 1992.
- MENDOZA MARIN, F.L.; *Modelagem, Simulação e Análise de Desempenho de Reatores Tubulares de Polimerização com Deflectores Angulares Internos*; Tese de Doutorado, FEQ/UNICAMP, Campinas, 2004.
- PAQUET, D.A. AND RAY, W.H.; *Tubular Reactors for Emulsion Polymerization: I and II, Experimental Investigation; Reactor, kinetics and catalysis and Model Comparison with Experiments*; *AIChE journal*, vol.40 No.1, January 1994.
- PATANKAR, S.V.; *Numerical Heat Transfer and Fluid Flow*; Hemisphere Publishing Corporation; New York, 1980.
- SCHOLTENS, C. A.; *Process Development for Continuous Emulsion Copolymerization*; CIP-DATA Library Technische Universiteit Eindhoven, Ter Verkrijging van de graad van Doctor, 2002.
- SIROLA, J.J. *Industrial Applications of Chemical Process Synthesis*, *AIChE*, Vol.23, 1-62, 1996.
- TOLEDO, E.C.V., *Modelagem, Simulação e Controle de Reatores Catalíticos de Leito Fixo*, Tese de Doutorado, FEQ/UNICAMP, Campinas, 1999.
- TUCKER III, C.L.; *Fundamentals of Computer Modeling for Polymer Processing*; Hanser Publishers, Munich Vienna New York, 1989.
- VERSTEEG, H.K. AND MALALASEKERA, W.; *An Introduction to Computational Fluid Dynamics, The Finite Volume Method*; 2nd Ed.; Addison Wesley Longman Limited; 1998.